

## Diffusion and stability of oxygen in GaAs and AlAs

Akihito Taguchi and Hiroyuki Kageshima

*NTT Basic Research Laboratories, 3-1 Morinosato-Wakamiya, Atsugi-shi, Kanagawa, 243-0198, Japan*

(Received 12 March 1999)

We investigated various basic properties of oxygen in GaAs and AlAs by using first-principles calculations and considering the charge states and Fermi-level effect. For GaAs, the obtained stable atomic configurations and their stability showed good agreement with experimentally obtained results. We found that many features, such as a stable site, a negative- $U$  nature, a charge-state-dependent diffusion path, and a rather high diffusion barrier height in the negatively charge state, are similar between GaAs and AlAs. Some features, however, were dependent on the host. We found that an asymmetry effect during the diffusion is pronounced in  $p$ -type host in both GaAs and AlAs, but the effect shows different characters depending on the host. O is more stable in AlAs than in GaAs. All of the obtained basic properties can be explained by three characteristics: the large electron negativity of oxygen, the strong O-Al bond, and the large polarization of AlAs hosts. From our theoretical study, the experimentally observed higher O concentration for AlAs layers in GaAs/AlAs systems can be clearly explained. [S0163-1829(99)06531-5]

### I. INTRODUCTION

Oxygen (O) is one of the most common contaminants of III-V semiconductors. Its high reactivity to other elements results in the formation of complex defects that reduce crystal quality. O forms deep carrier traps in the band gaps of GaAs and AlAs.<sup>1,2</sup> Because these features are not favorable for fabricating electronic devices, O is carefully removed during the processes for epitaxial growth and device fabrication. However, in a combined system of GaAs and AlAs, the AlAs layers were selectively oxidized and this is very useful feature for fabricating vertical-cavity surface-emitting lasers.<sup>3</sup> While the number of papers on selective oxidation has increased,<sup>4</sup> and the oxidation properties have been discussed in a phenomenological manner,<sup>5</sup> the microscopic oxidation mechanism is not clear yet.

The selective-oxidation property clearly shows that O has a higher reactivity to Al than to Ga. Another phenomenon that shows this higher reactivity can be seen in GaAs/AlAs superlattices. When such superlattices are grown, the concentration of O is much higher in the AlAs layers than in the GaAs layers.<sup>6</sup> This has been attributed to the incorporation of O atoms at the surface, but the diffusion properties have to also be considered, because diffusion modifies the spatial O distribution. The nature of this diffusion, however, has been little studied or discussed for GaAs either or AlAs.

To understand the selective oxidation and diffusion properties of O, it is necessary to understand the stable atomic configuration, its charge-state dependence, and its relative stability in GaAs and AlAs. Local-vibrational-mode (LVM) absorption measurement is a powerful method for investigating the atomic configurations. For O in GaAs, LVM measurements have been carried out, and several atomic configurations have been proposed. Two atomic configurations in particular, Ga-O-Ga and Ga-O-As, have been identified.<sup>7</sup> Because the Ga-O-Ga configuration shows a negative- $U$  nature, it has been studied in detail.<sup>8,9</sup> It had been thought that the O atom at the As site is the negative- $U$  center, but recent first-principles calculations showed that the interstitial O atom is

the center.<sup>10</sup> The characteristic properties of the other O centers in GaAs are little known. There have been no reports of LVM experiments for O in AlAs, so the stable atomic configuration of O in AlAs has not yet been clarified.

To clarify the basic properties of O in GaAs and AlAs, we investigated their stable sites, their charge-state dependence on the Fermi level, their diffusion properties, and their relative stability between the two hosts by using first-principles pseudopotential calculations. In the next section, the calculation method we used is briefly explained. In Sec. III, we discuss the stable sites and the stable charge state considering their Fermi level effect. The difference in O reactivity to Ga and to Al will also be discussed. Based on the obtained stable states, we estimated the diffusion paths and diffusion barrier heights. To estimate the relative stability of O in GaAs and AlAs, we calculated the energy relating to the O incorporation into the host. We found that O is more stable in AlAs than in GaAs.

### II. CALCULATION METHOD

The calculations were carried out within the local-density functional approximation. For Ga, Al, and As, soft pseudopotentials of the form proposed by Troullier and Martin were used.<sup>11,12</sup> Details of the pseudopotentials for Ga and As have already been published.<sup>12</sup> The pseudopotential for Al was checked by calculating the AlAs bulk properties.<sup>13</sup> The calculated lattice constant and bulk modulus show good agreement with the experimentally obtained ones. The calculated lattice constant is only 0.3% smaller than the experimental value. For O, the ultrasoft-pseudopotential developed by Vanderbilt<sup>14</sup> was used. This pseudopotential was previously applied to the Si system<sup>15</sup> and the GaAs system.<sup>10</sup> The pseudo-wave function was expanded by using a plane-wave basis set. A 32-atom supercell was used, and the lattice around the O atom was optimized. We used four  $k$  points to carry out the  $k$ -space integration. The kinetic-energy cutoff was taken to be 20.25 Ry. The convergence of the differences in the total energy between the different states was

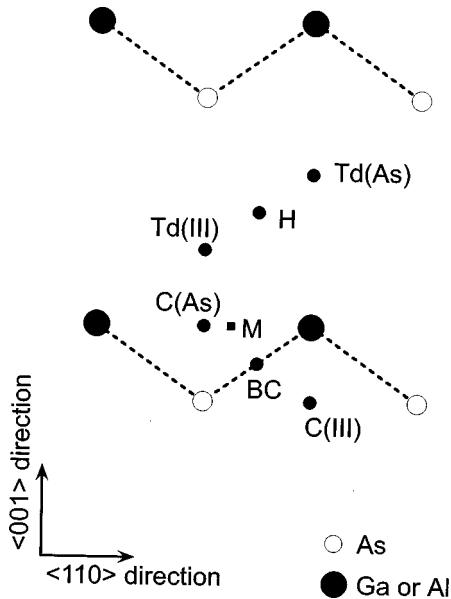


FIG. 1. Interstitial sites of GaAs and AlAs used to determine stable sites of O atoms. The (110) plane is shown. “Td(III)” denotes the tetrahedral interstitial site surrounded by group-III atoms. H is the hexagonal site, BC is the bond-center site, and AB is the antibonding site. C is the center of the rhombus formed by three adjacent lattice atoms and the nearest Td site. Since the M site, which is defined as the middle position between neighboring C(As) and C(III) sites, is not located on the (110) plane, its projected position on the plane is shown.

checked by calculations using a larger kinetic-energy cutoff of 36 Ry. The ambiguity in the relative total energy among the different states was estimated to be less than 0.15 eV, based on the calculated total energy difference between  $O^0$  and  $O^{2-}$  at the tetrahedral interstitial site. The conjugate-gradient technique was used to optimize both the electronic structure and the atomic configuration.<sup>16</sup> No symmetry was assumed in the optimization of the atomic configuration.

To determine the stable site of an O atom in GaAs and AlAs, we calculated the total energies at the various interstitial sites shown in Fig. 1. The H denotes the hexagonal interstitial site, and Td denotes the tetrahedral interstitial site. There are two kinds of Td sites in a zinc-blende structure, the one that exists depends on the kind of atoms at the nearest neighbor sites. The nearest neighbor atom is indicated in the parentheses. The III represents Ga on Al, depending on whether the lattice is GaAs or AlAs. The C site is the center of the rhombus composed by three adjacent lattice atoms and the nearest Td site. Because there are two kinds of C sites, the atom at the nearest neighbor is shown in the parentheses. The BC denotes the bond center site. The M denotes the middle between the neighboring C(As) and C(III) sites, but these sites are not on the same (110) plane. Considering the C(As) site in the figure, the nearest C(III) site is not on the (110) plane shown, but it is above (or below) the plane. Hence, the M site is not on the (110) plane shown, either. In the figure, its projected position is shown.

Because O can take several charge states, we considered several positive and negative charge states. The Fermi-level effect was also taken into account by calculating the formation energy.<sup>17</sup> In the calculations, the position of the O atom

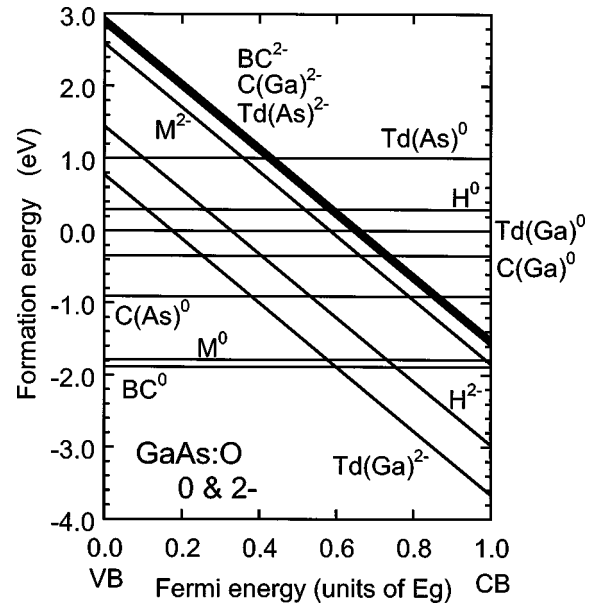


FIG. 2. Formation energy of an O impurity in GaAs as a function of the Fermi level for the neutral and  $-2$  charge states. The Fermi energy is measured by the calculated band gap of GaAs, and is taken to be zero at the top of the valence band. The energy for the Td(Ga) site in the neutral-charge state was taken as the energy reference.

was fixed at each site, except for the BC site, and then the positions of the surrounding atoms were optimized. For the BC site, the position of the O atom was optimized on the (110) plane, because the ideal BC site was found to be unstable and to give much higher energy than the relaxed BC site.

### III. RESULTS AND DISCUSSION

#### A. Stable site and stable-charge state

##### 1. In GaAs

For GaAs, we found that O takes four charged states, from  $+1$  to  $-2$ . Figure 2 shows the formation energy as a function of the Fermi level for the neutral and  $-2$  charge states in GaAs. The energies for the  $-1$  charge state are not shown because our previous calculations showed that this state is not the most stable at any Fermi level.<sup>10</sup> The energy for the Td(Ga) site in the neutral-charge state was taken as the reference energy. The Fermi energy was measured by calculating the bandgap of the GaAs. The top of the valence band was set at zero.

In the neutral-charge state, the most stable site is BC. At the BC site, an O atom forms bonds with adjacent Ga and As atoms, resulting in a Ga-O-As structure. The next most stable site is M, and its energy is very close to that of BC. The M site is close to the BC site, and the O atom also takes the Ga-O-As structure. These two sites would practically be the same. Since the lattice was relaxed under the limited conditions in the present calculations [the O atom position was fixed in the calculation for the M site, and for the BC site the O atom position was relaxed within the (110) plane], if the atomic configurations including the position of the O atom were fully optimized, the two optimized configurations from

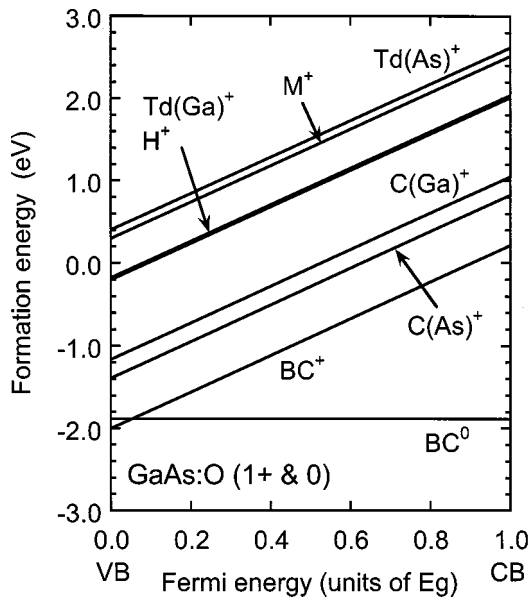


FIG. 3. Formation energy of an O impurity in GaAs as a function of the Fermi level for the +1 charge state. For the neutral-charge state, the energy of the most stable site of BC is shown. The reference energy is the same as that in Fig. 2.

BC and M would possibly be the same.

The next stable site is C(As). More detailed calculations including the optimization of the O atom position around C(As) site showed that at a slightly different position from C(As) is the local minimum.<sup>10</sup> The O atom moved along the  $\langle 100 \rangle$  direction to form a Ga-O-Ga structure. This structure showed a negative- $U$  nature, and has already been discussed.<sup>7,8,10</sup>

Other sites, such as C(Ga), Td(Ga), H, and Td(As), are not metastable states, judging from the calculated forces. Moreover, because an energy barrier was found between the Ga-O-As configuration (M and BC) and the Ga-O-Ga configuration [near C(As)], the present calculations suggest that these two configurations are achieved in GaAs in the neutral-charge state. Such two stable configurations were observed in LVM experiments conducted on O-doped semi-insulating GaAs samples.<sup>7</sup> The two sets of LVM signals were observed at around  $715$  and  $845$   $\text{cm}^{-3}$ , and they were attributed to the Ga-O-Ga and Ga-O-As structures.<sup>7,8</sup> Because the O atom is expected to be neutral in such semi-insulating samples, the stable sites calculated are consistent with the experimental observations.

As the Fermi level rises from the top of the valence band to the bottom of the conduction band, the most stable charge-state changes from 0 to  $-2$ . Figure 2 clearly shows that O forms a deep level in the GaAs bandgap, which is qualitatively consistent with the experimental observations.<sup>1</sup> In the  $-2$  charge state, the Td(Ga) site is the most stable. More detailed calculations have shown that the most stable site is slightly different from the Td(Ga) site and takes a Ga-O-Ga structure (the negative- $U$  center).<sup>10</sup>

The energy for the other Td site, Td(As), is larger than that for Td(Ga). This can qualitatively be understood by considering electron negativity. Because the electron negativity of Ga is smaller than that of As, when O, which has the largest electron negativity among these three elements, becomes negatively charged, it prefers a site surrounded by As

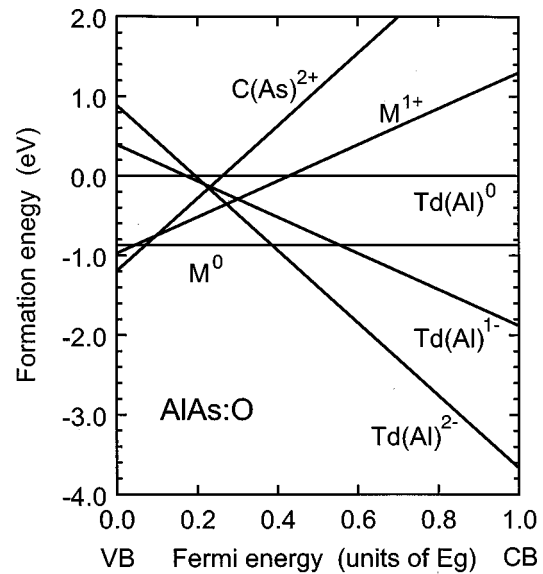


FIG. 4. Formation energy as a function of Fermi level for the most stable sites of charge states from +2 to  $-2$ . The energy of the Td(Al) in the neutral-charge state was taken as the reference energy. The Fermi energy was taken as zero at the top of the valence band and measured by calculating the AlAs bandgap.

atoms to one surrounded by As atoms. As a result, the Td(Ga) site is more stable than the Td(As) site. The reason the energies for the BC and C(Ga) sites are rather high can be understood in the same manner.

Figure 2 shows that the Ga-O-As configuration (BC and M) is more stable in the neutral charge state than in the negatively charged state at any Fermi level, indicating that the Ga-O-As center does not capture electrons. This result is consistent with light illumination experiments. The light illumination is a widely used in experiments to change the charge state. Although the  $715$   $\text{cm}^{-1}$  LVM signal (due to the negative- $U$  center<sup>8,10</sup>) is very sensitive to illumination, the  $845$   $\text{cm}^{-1}$  LVM signal (due to the Ga-O-As center) is not.<sup>18</sup> This clearly indicates that an O center taking the Ga-O-As configuration does not capture electrons, being consistent with our calculation results.

Figure 3 shows the formation energies as a function of the Fermi level for the neutral and +1 charge states in GaAs. For the neutral-charge state, only the result for the most stable site of BC is shown to avoid complexity. When the Fermi level is at the top of the valence band, the energy for the BC site in the +1 charge state is slightly lower than that in the neutral-charge state. It can be said that the capability of the O center for capturing a hole is small in GaAs.

## 2. In AlAs

For O in AlAs, we carried out similar calculations. The results indicate that O takes five charge states, ranging from +2 to  $-2$  in AlAs. Different sites become the most stable depending on the charge state. For the +2 charge state, the C(As) site is the most stable. The M site is the most stable for the +1 and neutral-charge states. For the  $-1$  and  $-2$  charge states, the Td(Al) site is the most stable.

Figure 4 shows the formation energies of the most stable

sites for each charge state. The Fermi level was measured by calculating the AIAs band gap. The energy for the Td(Al) site in the neutral-charge state was taken as the reference energy. Although O may take five charge states in AIAs, the +1 and -1 charge states are not stable at any Fermi level. The figure clearly shows that the -1 charge state is the metastable state. Oxygen shows a negative- $U$  nature in AIAs when its charge states are changed among 0, -1, and -2. In the charge-state change among +2, +1, and 0, the O may also show a negative- $U$  nature, but it is not so obvious because the energies near the cross points of these three states are quite close.

Figure 5(a) shows the formation energy of the various sites for the neutral-charge state and the -2 charge state. The results for the -1 charge state are not shown, since the -1 charge state is a metastable state, as shown in Fig. 4. In the neutral charge state, the M, C(As), and BC sites have quite close formation energies. If the lattice was fully relaxed, the optimized atomic configurations from these three sites might have been the same. As the Fermi level rises, the -2 charge state becomes the most stable. This clearly shows that an Al atom forms a deep level in AIAs, which was suggested by the experimental results.<sup>2</sup>

The most stable site in the -2 charge state is Td(Al), while the other Td site of Td(As) has the much higher energy. This tendency is the same as that observed for GaAs (Fig. 2) and can also be qualitatively understood in the same way by considering the electron negativity. The relative magnitude of the electron negativity is that  $O > As > Al$ . Therefore, the O atom favors a site surrounded by Al atoms than a site surrounded by As atoms. The reason the energies for M, C(Al), and BC are rather high can also be qualitatively explain in the same manner.

Figure 5(b) shows the formation energy for the neutral-charge state and the +2 charge state. The results for the +1 charge states are not shown, since the +1 charge state is not stable, as shown in Fig. 4. For the neutral-charge state, only the result for the M site is shown for simplicity. Except for the Td(As) site, the energies are close to each other. The rather stable sites are BC, M, and C(As); they are in the spatial region where the valence electron density is rather high. This is quite natural because due to the large electron negativity, an O atom prefers the high valence-electron-density region to compensate for the electron shortage in the +2 charge state.

Our investigation of the stable sites of an O atom indicated that the most stable site and its dependence on the charge state are similar for GaAs and AIAs. However, O tends more to couple with Al than with Ga. This nature can be observed when the bonding nature is examined in detail. For the neutral-charge state, the BC site is rather stable in both GaAs and AIAs. At the BC site, O takes the Ga(Al)-O-As configuration. In GaAs, the estimated bond lengths of O-Ga and O-As were the same (1.78 Å), while, in AIAs, the estimated bond lengths of O-Al and O-As are different. The O-Al bond length of 1.64 Å is shorter than the O-As bond length of 1.76 Å. The shorter bond length of O-Al may be deduced from the rather strong coupling of O with Al. In the -2 charge state, this strong coupling was seen in the atomic configuration for the Td(III) site as the shorter distance between O and Al than that between O and Ga. The distance of

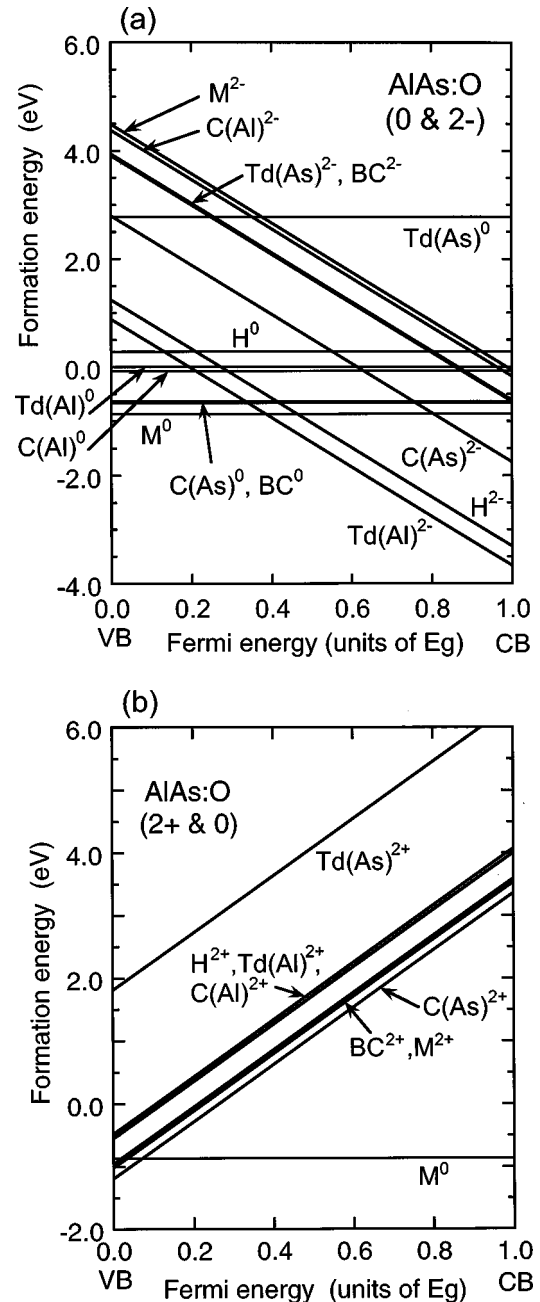


FIG. 5. Formation energy of an O impurity in AIAs as a function of Fermi level for (a) the neutral and -2 charge states, and (b) the neutral and +2 charge states. The Fermi energy was measured by calculating the band gap of AIAs and was taken to be zero at the top of the valence band. The Td(Al) site in the neutral-charge state was taken as the energy reference. In (b), the energies of some sites are not shown to simplify the figure.

O-Al in AIAs is 2.02 Å, while that of O-Ga in GaAs is 2.10 Å.

## B. Diffusion path and diffusion barrier height

### 1. Diffusion in $n$ -type hosts (negatively charged state)

The calculation results presented in the previous section indicate that O takes a -2 charge state in  $n$ -type hosts for both GaAs and AIAs. In the negatively charged state, the sites in the low valence-electron-density region are rather

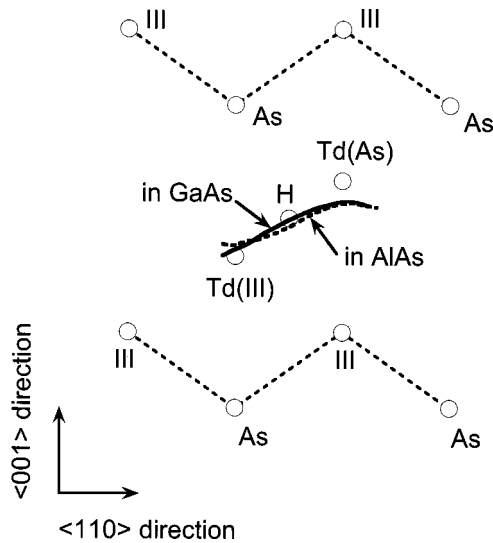


FIG. 6. Obtained O atom diffusion paths in GaAs and AlAs for  $-2$  charge state. The solid line is the path in GaAs, and the dotted line is that in AlAs. The open circles are ideal lattice sites and some high-symmetry sites. The lattice was relaxed, but the relaxed atom positions are not shown.

stable. Therefore, the diffusion path of an O atom may basically be  $-Td(III)-H-Td(As)-H-Td(III)-$  in both hosts. The diffusion-energy barrier heights were estimated by calculating the total energy along this path. To estimate the diffusion path and the diffusion barrier height, we moved an O atom within the  $(110)$  plane. It was moved from the H site toward the Td(III) and Td(As) sites. We moved it slightly in the  $\langle 110 \rangle$  direction and fixed the coordinate in the  $\langle 110 \rangle$  direction. Then, its position along the  $\langle 001 \rangle$  direction was optimized. The positions of the other atoms were fully optimized. Figure 6 shows the estimated diffusion paths in GaAs and AlAs. The O atoms clearly diffuse in the low valence-electron-density region. The diffusion paths are quite similar in GaAs and AlAs, as expected.

The total energies along the diffusion paths are shown in Fig. 7(a) for GaAs and Fig. 7(b) for AlAs. The arrows in the figures indicate the positions in the  $\langle 110 \rangle$  direction of the sites indicated. The lowest energy along the diffusion path was taken as the reference energy in each host. In GaAs [Fig. 7(a)], the energy monotonically increases when the O atom moves from the Td(Ga) site toward the Td(As) site. The energy shows a peak near the Td(As) site. Defining the diffusion barrier height as the energy difference between the minimum energy and the maximum energy, we obtained 2.0 eV. In AlAs [Fig. 7(b)], the position that gives the minimum energy is shifted from zero in the  $\langle 110 \rangle$  direction, which differs from the GaAs case. This may be because an O atom forms stronger bonds with Al atoms than with Ga atoms. As an O atom approaches the Td(As) site, the energy increases, and the energy maximum is given near the Td(As) site. The estimated diffusion barrier height was 3.4 eV. Although the diffusion barrier height of O has not been experimentally obtained in GaAs and AlAs, it was reported in Si as 2.44 eV.<sup>19</sup> The estimated barrier height in GaAs is comparable to this value, while that in AlAs is much larger. The O barely diffuses in AlAs when it takes a  $-2$  charge state.

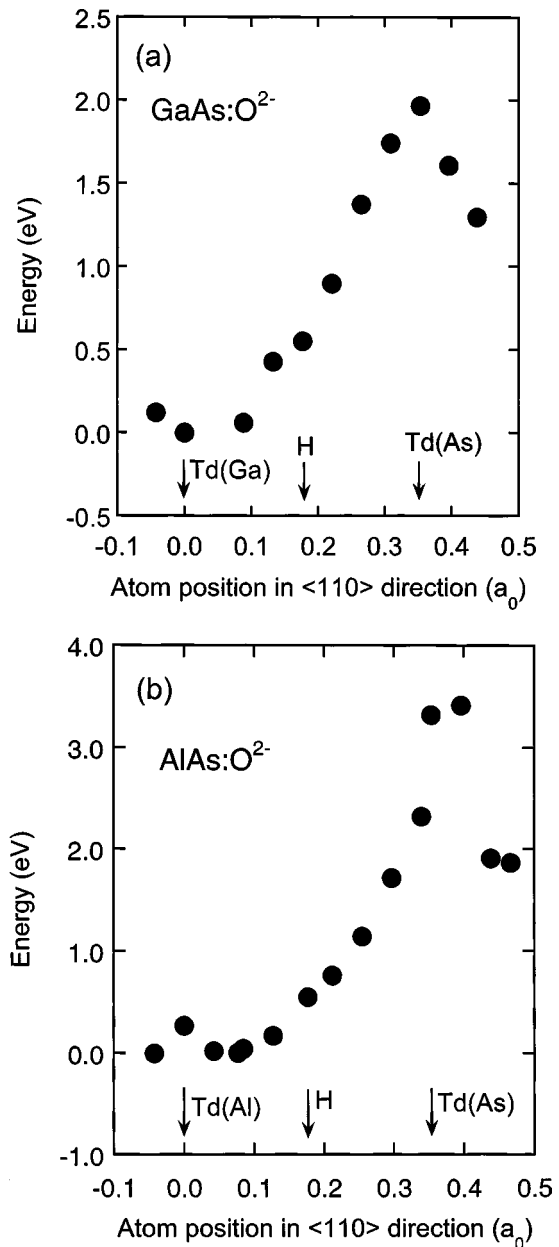


FIG. 7. Total energies along the diffusion path for the  $-2$  charge state in (a) GaAs and (b) AlAs. In each figure, the lowest energy was taken as the energy reference. Arrows show the positions in the  $\langle 110 \rangle$  direction of the sites indicated. The O atom position in the  $\langle 110 \rangle$  direction was measured using lattice constant  $a_0$ , and the position of the Td(III) site was defined as the origin.

Although the diffusion paths and the energy profiles are similar in GaAs and AlAs, the diffusion barrier in AlAs is much higher. The minimum energy is given near Td(III), and the maximum energy is given near Td(As) in both hosts. As can be seen in Figs. 2 and 5(a), the energy difference between the Td(III) site and the Td(As) site is larger in AlAs than in GaAs. The higher barrier in AlAs is deduced from this nature. When the O atom occupies the Td(As) site and takes a  $-2$  charge state, the distance between the O atom and the nearest neighbor As atoms is 2.42 Å in GaAs and 2.67 Å in AlAs. In GaAs, the O-As distance is close to the GaAs bond length of the bulk, which is 2.45 Å, while in AlAs the O-As distance is much larger. In AlAs, a repulsive force

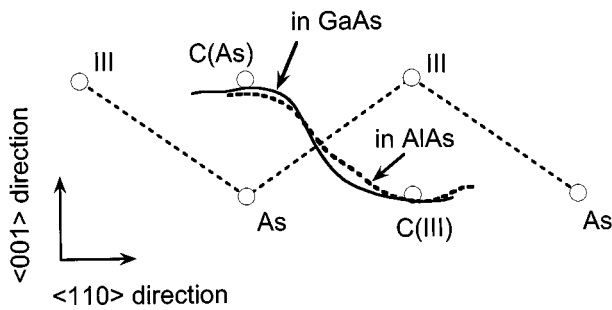


FIG. 8. Obtained O-atom diffusion paths for positively charged state in GaAs and AlAs. The solid line is the path in GaAs, and the dotted line is that in AlAs. The open circles are the ideal lattice sites and symmetric C sites. The lattice was relaxed, but the relaxed positions are not shown.

seems to work between the O atom and the neighboring As atoms. This repulsive force may be due to the polarization of the host. Because the polarization of the Al-As bond in AlAs is larger than that of the Ga-As bond in GaAs, the As atoms are more negative in AlAs than in GaAs. Therefore, the repulsive force between the As atoms and the negatively charged O atom is larger in AlAs. As a result, the O-As distance is larger in AlAs, implying a larger strain in AlAs than in GaAs. A larger strain enlarges the energy, resulting in a higher diffusion barrier.

## 2. Diffusion in *p*-type hosts (positively charged state)

The formation energies shown in Figs. 3 and 5(b) indicate that an O takes the positive charge state of +1 in GaAs and +2 in AlAs in *p*-type hosts. The stable sites are different from those in *n*-type hosts (−2 charge state), indicating that the diffusion paths are also different. In both hosts, the low energy sites are BC, C(As), and C(III). Therefore, the migration path may be basically the same in both hosts, and it may be  $-BC-C(III)-BC-C(As)-BC-$ . The procedure for determining the diffusion path and the diffusion barrier height was the same as that used in the *n*-type hosts, but the O atom was moved from the relaxed BC site. Figure 8 shows the estimated diffusion paths in GaAs and AlAs when the O is positively charged. The surrounding atom positions were relaxed, but the ideal lattice sites are shown in the figure. The O atoms clearly move via the high valence-electron-density region. The diffusion paths are quite similar in both hosts, as expected.

Figure 9 shows the calculated energies along the diffusion path for GaAs. The BC site in the  $\langle 110 \rangle$  direction denoted by the arrow corresponds to the ideal BC site. A notable feature is that the energy profile is not symmetric around the C(As) and C(Ga) sites. This is due to an asymmetric effect and will be discussed later. Near the ideal BC site, the potential shows a local peak, indicating that the Ga-As bond acts as a barrier during the diffusion. The diffusion-energy barrier height was estimated as the difference between the minimum and maximum energy, and it is 0.92 eV.

The diffusion barrier height is conventionally estimated by comparing the energies at various symmetrical sites, then estimating the barrier height as the energy difference between two appropriate sites. However, when the impurity atom and the lattice atoms interact with each other, the lattice

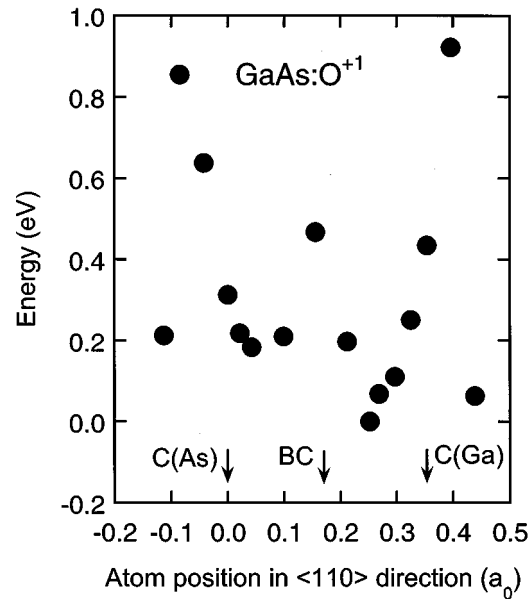


FIG. 9. Total energy during diffusion in GaAs for +1 charge state. The lowest energy was taken as the energy reference. The BC site denoted by the arrow is the ideal BC site position.

atoms cannot hold their original symmetry during the diffusion. In O in Si, the theoretical calculations including the asymmetry effect show good agreement with the experimentally obtained diffusion barrier height.<sup>20</sup> To obtain a reliable barrier height, the asymmetry effect has to be included. The estimation method we used includes the asymmetry effect. As a result, the potential profile is not symmetric around the C(As) and C(Ga) sites. The asymmetry effect is not pronounced in the negatively charged state because the O atoms diffuse in the low valence-electron-density region, where the distances between the O atom and the neighboring atoms are rather large and the O atom does not form bonds with the lattice atoms. In contrast, in the positively charged state, because the O atom forms bonds with the lattice atoms and such bonds have to be broken during diffusion, the asymmetry effect cannot be ignored.<sup>21</sup> The asymmetric potential profile around the C(Ga) and C(As) sites in Fig. 9 clearly shows that the effect is important in determining the diffusion barrier height.

To investigate this effect, we plotted the positions of the nearest neighbor Ga and As atoms during the diffusion. As shown in Fig. 10, the O atom was moved from the relaxed BC site, which was the start position and is not shown in the figure, to positions 1, 2, and 3. The solid lines between the atoms are guides. At position 1, the O takes the Ga-O-As structure. At position 2, the distance to the Ga atom on the right side (1.87 Å) is shorter than to the Ga atom on the left side (2.18 Å). The O atom seems to form a stronger bond with the right-side Ga atom than with the left-side Ga atom, although the O atom is on the left side of the C(As) site. The As atom position becomes far from the ideal As lattice site. At position 3, a bond exchange occurs. The O breaks its bond with the right-side Ga atom and forms a bond with the left-side Ga atom. The As atom jumps to a position near the ideal As lattice site. Among the three configurations shown in the figure, the configuration for when the O atom is at

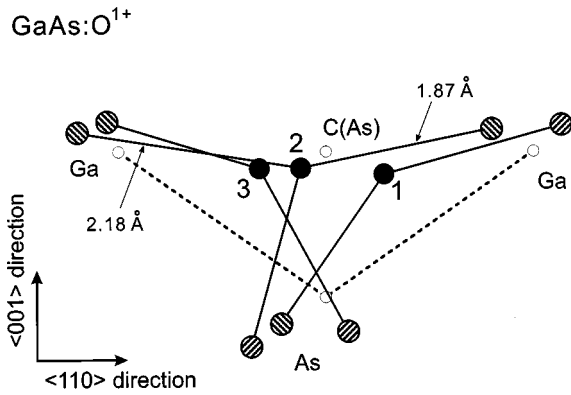


FIG. 10. Relaxed atom positions of neighboring Ga and As atoms during diffusion for several O positions near C(As) site. Open circles are the ideal lattice sites and the C(As) site. Filled circles represent the O atom. Hatched circles represent the relaxed Ga and As atoms. Solid lines are drawn between the corresponding O, Ga, and As atoms as guides.

position 2 is expected to have the largest strain. Therefore, the energy profile is expected to be asymmetric around the C(As) site; an asymmetric nature was actually obtained, as shown in Fig. 9. The similar configuration change was seen around the C(Ga) site. If the asymmetry effect was ignored and the barrier height was estimated as the energy difference between the energies at the BC and C(Ga) sites, the barrier height is 0.84 eV. The asymmetry effect enlarges the barrier height by 0.08 eV.

As shown in Fig. 8, the O diffusion path in AlAs is quite similar to that in GaAs. The energy profile during the diffusion was calculated and is shown in Fig. 11. Two features were similar to those seen in GaAs: the energy maximum at a site beyond the C(Al) site due to the asymmetry effect and the Al-As bond acts as a diffusion barrier. The potential profile around the C(As) site, however, is apparently different from that in GaAs. The C(As) site is at the bottom of the

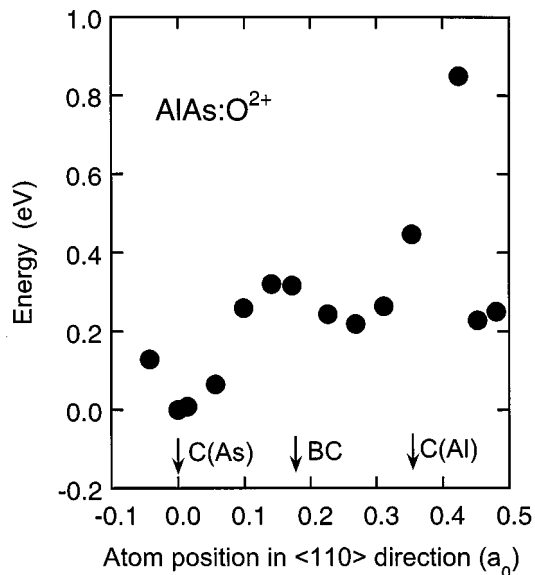


FIG. 11. Total energies during diffusion in AlAs for +2 charge state. The lowest energy was taken as the energy reference.

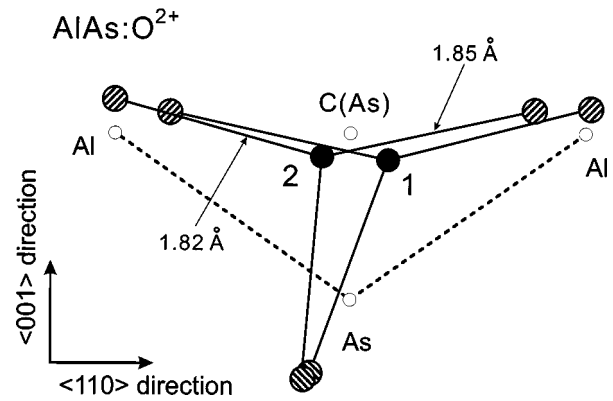


FIG. 12. Relaxed atomic configurations of an O atom and neighboring Al and As atoms near the C(As) site during the diffusion. Open circles are the ideal lattice sites and the C(As) site. Filled circles represent the O atom. Hatched circles represent the relaxed Al and As atoms. Solid lines are drawn between the corresponding O, Al, and As atoms as guides.

potential well, indicating that the asymmetry effect is weak around this site.

The weak asymmetry effect around the C(As) site is due to the bonding nature of O to Al. The atomic configurations around the C(As) site are shown in Fig. 12. The O atom seems to form bonds with two neighboring Al atoms. At position 2, which has the same coordinate in the  $\langle 110 \rangle$  direction as position 2 in Fig. 10, the distances from the O atom to the two neighboring Al atoms are 1.85 and 1.82 Å, which are nearly the same. The interactions of the O atom with the two neighboring Al atoms seem to be almost the same. Moreover, the Al-O-Al configuration is almost symmetric between positions 1 and 2, as can be seen in the figure. Therefore, the total energy mainly depends on the O-Al configuration and weakly depends on the O-As configuration, resulting in the weak asymmetric effect around the C(Al) site. The estimated diffusion barrier height in AlAs is 0.84 eV. If the asymmetry effect around the C(Al) site was neglected and the barrier was estimated to be the energy difference between the C(Al) and the C(As) sites, the barrier is 0.64 eV. The asymmetry effect enlarges the barrier height by 0.2 eV.

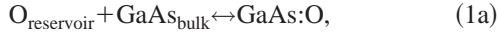
The estimated barrier heights in the positively charged state in GaAs and AlAs are much smaller than those in  $n$ -type hosts ( $-2$  charge state). This finding suggests that if the O takes the positively charged state, it will easily diffuse in the host.

### C. Relative stability

O incorporates easier into AlAs than into GaAs. As mentioned, in GaAs/AlAs superlattices, the O concentration is much higher in the AlAs layers than in the GaAs layers. We discussed the diffusion in GaAs and AlAs in the previous section and we showed that in both hosts the  $-2$  charge state is the most stable over a wide range of Fermi levels and that the diffusion barrier is much higher in AlAs than in GaAs. The estimated barrier heights seem to be consistent with the concentration profile of O in GaAs/AlAs superlattices because the lower barrier height in GaAs indicates that O atoms diffuse from the GaAs layers to the AlAs layers. However, to

understand the concentration profile, the relative stability in GaAs and AlAs has to be taken into account, because if O is much more stable in GaAs, it remains in GaAs layers.

To investigate the relative stability, we considered the following incorporation reactions:



We assumed a common reservoir for O ( $O_{\text{reservoir}}$ ). The right-hand sides of the equations express the states where an O atom is incorporated in the host. We did not consider the incorporation process at the surface. Because the diffusion and relative stability mainly determine the concentration profile after the incorporation of O atoms, the details of the incorporation process at the surface are not essential to understand the profile in the GaAs/AlAs system. The reaction energy,  $E_R$ , was defined as the energy difference between the right-hand and left-hand sides of the reaction:

$$E_R^{\text{GaAs}} \equiv E(\text{GaAs}:\text{O}) - [E(O_{\text{reservoir}}) + E(\text{GaAs}_{\text{bulk}})], \quad (2a)$$

$$E_R^{\text{AlAs}} \equiv E(\text{AlAs}:\text{O}) - [E(O_{\text{reservoir}}) + E(\text{AlAs}_{\text{bulk}})]. \quad (2b)$$

Further, the difference between the reaction energies was defined as

$$\Delta E_R \equiv E_R^{\text{GaAs}} - E_R^{\text{AlAs}} = E(\text{GaAs}:\text{O}) - E(\text{AlAs}:\text{O}) \\ - [E(\text{GaAs}_{\text{bulk}}) - E(\text{AlAs}_{\text{bulk}})].$$

Because the common reservoir was assumed, this equation does not contain the O reservoir energy. If  $\Delta E_R$  is positive, O is more stable in AlAs than in GaAs.

In the above equations, the charge states are not shown in order to make the formulations simple, but the most stable charge state depends on the Fermi level, as already shown. The most stable sites are also different in GaAs and AlAs. Therefore,  $\Delta E_R$  was estimated considering these effects for  $n$ -type ( $-2$  charge state) and  $p$ -type hosts ( $+1$  charge state for GaAs and  $+2$  charge state for AlAs), separately. The values obtained were  $+1.7$  eV for  $n$ -type hosts and  $+0.77$  eV for  $p$ -type hosts, being positive in both conduction types. Therefore, an O atom is more stable in AlAs than in GaAs regardless of the host conduction type.

Assuming that the potential barrier from the AlAs layer to the GaAs layer can be roughly estimated as the sum of  $\Delta E_R$  and the diffusion barrier height, it is  $3.7$  eV for  $n$ -type GaAs/AlAs systems and  $1.7$  eV for  $p$ -type GaAs/AlAs systems. Considering the very large potential barrier for  $n$ -type systems and the large diffusion barrier in  $n$ -AlAs, the O barely moves from the AlAs layers to the GaAs layers. This is

consistent with the experimental observations. For  $p$ -type systems, however, the potential barrier is not so high. If GaAs/AlAs superlattices with  $p$ -type conductivity are grown, the O concentration distribution may be broad.

#### IV. SUMMARY

We have investigated the basic properties of O in GaAs and AlAs, such as the stable sites, the diffusion properties, and the relative stability, by using first-principles calculations and considering the Fermi-level effect. Our calculations suggest two atomic configurations, Ga-O-Ga and Ga-O-Al, for GaAs. Two such configurations were actually observed in the LVM measurements. They also suggest that O shows a negative- $U$  nature also in AlAs, as was experimentally observed in GaAs.

The diffusion paths and the diffusion barrier heights were estimated by including the asymmetry effect. The basic diffusion features, such as the diffusion path and its charge-state dependence, are the same in GaAs and AlAs. In the negatively charged state, the O atom diffuses in the low valence-electron-density region, while in the positively charged state, it diffuses in the high valence-electron-density region. We found that the diffusion barrier heights are much lower in the positively charged state than in the negatively charged state in both hosts. This means that O diffuses much easier in  $p$ -type hosts. By examining the potential profile and the atomic configuration during diffusion, we found that the asymmetry effect is more pronounced in the positively charged state.

We also estimated the relative stability of O in GaAs and AlAs considering the reaction energy difference. We found that an O atom is more stable in AlAs than in GaAs regardless of the host conduction type. The high potential barrier from AlAs to GaAs for  $n$ -type hosts suggests that O atoms barely move to GaAs layers, consistent with experimental observations. The estimated rather low potential barrier for  $p$ -type hosts suggests a broader O-concentration profile in  $p$ -type GaAs/AlAs systems.

We found that the basic properties of O in GaAs and AlAs can be qualitatively understood from three characteristic features: the large electron negativity of O, the stronger O bond with Al than with Ga, and the larger polarization of AlAs hosts than GaAs hosts.

#### ACKNOWLEDGMENTS

The authors would like to thank to Dr. Kenji Shiraishi, Dr. Kazumi Wada, and Dr. Chikara Amano for their fruitful discussions. They also thank Dr. Takahisa Ohno for his discussions on the pseudopotential of Al and the bulk properties of AlAs. They acknowledge the critical reading of the manuscript by Dr. Yoshiro Hirayama.

<sup>1</sup>M. D. Sturge, Phys. Rev. **127**, 768 (1962); A. L. Lin, E. Omelianovski, and R. H. Bube, J. Appl. Phys. **47**, 1852 (1976); J. Lagowski, D. G. Lin, T. Aoyama, and H. C. Gatos, Appl. Phys. Lett. **44**, 336 (1984).

<sup>2</sup>C. Amano, K. Ando, and M. Yamaguchi, J. Appl. Phys. **63**, 2853

(1988); M. S. Goorsky, T. F. Kuech, F. Cardone, P. M. Mooney, G. J. Scilla, and R. M. Potemski, Appl. Phys. Lett. **58**, 1979 (1991); M. Hata, H. Takata, T. Yano, N. Fukuhara, T. Maeda, and Y. Uemura, J. Cryst. Growth **124**, 427 (1992).

<sup>3</sup>D. L. Huffaker, D. G. Deppe, K. Kumar, and T. J. Rogers, Appl.



- Phys. Lett. **65**, 97 (1994); K. L. Lear, K. D. Choquette, R. P. Schneider, Jr., S. P. Kilcoyne, and K. M. Geib, *Electron. Lett.* **31**, 208 (1995); Y. Hayashi, T. Mukaiharu, N. Hatori, N. Ohnoki, A. Matsutani, F. Koyama, and K. Iga, *ibid.* **31**, 560 (1995); G. M. Yong, M. H. MacDougal, and P. D. Dapkus, *ibid.* **31**, 886 (1995); N. M. Margalit, D. I. Babic, K. Streubel, R. P. Mirin, D. E. Mars, J. E. Bowers, and E. L. Hu, *Appl. Phys. Lett.* **69**, 471 (1996).
- <sup>4</sup>W. T. Tsang, *Appl. Phys. Lett.* **35**, 426 (1978); A. R. Sugg, E. I. Chen, T. A. Richard, N. Holonyak, Jr., and K. C. Hsieh, *ibid.* **62**, 1259 (1993); *J. Appl. Phys.* **74**, 797 (1993); T. Yoshikawa, H. Saito, H. Kosaka, Y. Sugimoto, and K. Kasahara, *Appl. Phys. Lett.* **72**, 2310 (1998).
- <sup>5</sup>M. Ochiai, G. E. Giudice, H. Termkin, J. W. Scott, and T. M. Cokerill, *Appl. Phys. Lett.* **68**, 1898 (1996); R. L. Naone and L. A. Coldren, *J. Appl. Phys.* **82**, 2277 (1997); B. Koley, M. Dagenais, R. Jin, J. Pham, G. Simonis, G. McLane, and D. Stone, *ibid.* **82**, 4586 (1997).
- <sup>6</sup>T. Someya, H. Akiyama, Y. Kadoya, T. Noda, T. Matsusue, H. Noge, and H. Sakaki, *Appl. Phys. Lett.* **63**, 1924 (1993).
- <sup>7</sup>C. Song, W. Ge, D. Jiang, and C. Hsu, *Appl. Phys. Lett.* **50**, 1666 (1987); X. Zong, D. Jang, W. Ge, and C. Song, *ibid.* **52**, 628 (1988); J. Schneider, B. Dischler, H. Seelewind, P.M. Mooney, J. Lagowski, M. Matsui, D. R. Beard, and R. C. Newman, *ibid.* **54**, 1442 (1989).
- <sup>8</sup>H. Ch. Alt, *Phys. Rev. Lett.* **27**, 3421 (1990).
- <sup>9</sup>M. Skowronski, S. T. Neild, and R. E. Kremer, *Appl. Phys. Lett.* **57**, 902 (1990).
- <sup>10</sup>A. Taguchi and H. Kageshima, *Phys. Rev. B* **57**, R6779 (1998).
- <sup>11</sup>N. Troullier and J. Martins, *Phys. Rev. B* **43**, 1993 (1991).
- <sup>12</sup>H. Kageshima and K. Shiraishi, *Phys. Rev. B* **56**, 14 985 (1997).
- <sup>13</sup>T. Ohno (private communications).
- <sup>14</sup>D. Vanderbilt, *Phys. Rev. B* **41**, 7892 (1990); J. Yamauchi, M. Tsukada, S. Watanabe, and O. Sugino, *Surf. Sci.* **341**, L1037 (1995).
- <sup>15</sup>H. Kageshima and K. Shiraishi, in *23rd International Conference on Physics and Semiconductors*, edited by M. Scheffler and R. Zimmermann (World Scientific, Singapore, 1996), pp. 305 and 903.
- <sup>16</sup>M. P. Teter, M. C. Payne, and D. C. Allen, *Phys. Rev. B* **40**, 12 255 (1989); O. Sugino and A. Oshiyama, *Phys. Rev. Lett.* **68**, 1858 (1992).
- <sup>17</sup>L. Pabesi and P. Giannozze, *Phys. Rev. B* **46**, 4621 (1992).
- <sup>18</sup>H. Ch. Alt (private communications).
- <sup>19</sup>J. C. Mikkelsen, Jr., *Appl. Phys. Lett.* **40**, 336 (1982).
- <sup>20</sup>M. Ramanoorthy and S. T. Pantelides, *Phys. Rev. Lett.* **76**, 267 (1996).
- <sup>21</sup>For O in Si, the most stable site is BC and the diffusion was thought to be the jump to the neighboring BC site. Because the bonds between Si and O atoms are formed at the BC site, the asymmetry effect cannot be ignored.